Available online at www.sciencedirect.com
SCIENCE DIRECT®
International Journal of Solids and Structures 42 (2005) 1537–1545
INTERNATIONAL JOURNAL OF SOLIDS and STRUCTURES
www.elsevier.com/locate/ijsolstr

Stiffness of a curved beam subjected to axial load and large displacements

Carlos González *, Javier LLorca

Department of Materials Science, Polytechnic University of Madrid, E.T.S. de Ingenieros de Caminos, 28040 Madrid, Spain

Received 29 April 2004; received in revised form 20 August 2004
Available online 13 October 2004

Abstract

The deformation of an inextensible, curved elastic beam subjected to axial load is studied using the Bernouilli–Euler hypothesis and including the effect of large displacements. The axial displacement of the beam was expressed as a function of the axial load in terms of two incomplete elliptic integrals and contained a singularity as the beam was fully straightened. The nature of the singularity was determined and the load–axial displacement curves were accurately fitted to a rational expression with the same type of singularity, which provides an analytical expression for the evolution of the beam stiffness during deformation. Another analytical expression (although implicit) was obtained in the case of extensible beams, where the elongation due to normal stresses cannot be neglected. These results are relevant to the simulation of the elastic deformation of non-woven felts.

Keywords: Elasticity; Beam theory; Composites; Non-woven fabrics

1. Introduction

Non-woven fabrics are a cost-effective type of low density felts in view of the easy and high speeds of their manufacture, which greatly exceed those attainable by knitting and weaving machines. Non-woven felts and sheets made up of polyethylene fibers have found many applications in the construction and packaging industries and protective apparel against corrosive liquids and harmful particles (E.I. DuPont de Nemours Inc., 2004; DSM, 2004). Moreover, the structure of polyethylene fiber felts leads to an outstanding tear resistance and energy absorption capability, and they perform exceptionally well to protect against

* Corresponding author. Tel.: +34 913 365 375; fax: +34 915 437 845.
E-mail addresses: cgonzalez@mater.upm.es (C. González), jllorca@mater.upm.es (J. LLorca).

0020-7683/$ - see front matter © 2004 Elsevier Ltd. All rights reserved.
doi:10.1016/j.ijsolstr.2004.08.018

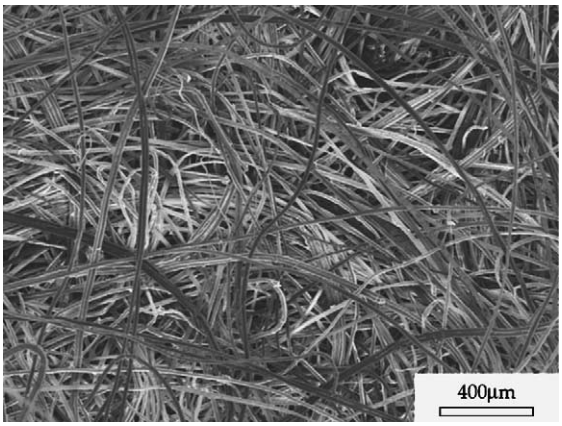

Fig. 1. Scanning electron micrograph of a polyethylene felt showing the network of curved fibers which make up the structure.

fragments of exploding bombs. Polyethylene felts are manufactured by depositing the short fibers into a mat which is consolidated by thermal, mechanical or chemical mechanisms to induce bonds at filament crossover points, providing a self-sustaining structure. The microstructure of the felt is made up of a network of curved fibers linked to each other (Fig. 1). This provides a very flexible structure under in-plane deformation as the fibers are progressively straightened (Chocrón et al., 2002). The initial stiffness depends obviously on the characteristics of the fiber network (felt density, fiber orientation, number of bonds per unit area, etc.) and on the stiffness of the curved fibers. Many models have been developed in the past (mainly in the paper community) to account for the influence of the above parameters but they always assumed that the fibers behave as elastic Bernouilli–Euler or Timoshenko beams within the framework of the small displacements theory (Cox, 1952; Van den Akker, 1962; Ostoja-Starzewski and Stahl, 2000; Perkins, 2001). While this is a good approximation for paper and other felts made up of straight fibers, the low initial modulus of the polyethylene felts is controlled by the stiffness of the folded fibers which is significantly lower than that of straight ones and varies in several orders of magnitude during deformation as a result of the shape change.

The elastic deformation of a cantilever beam including the effect of large displacements was first addressed by Bisshopp and Drucker (1945) for the particular case of a concentrated load perpendicular to the beam axis, and various results of the deformation of elastic cantilevers expressed in terms of elliptic integrals can be found in Frisch-Fay (1962). Numerical solutions for the deformation of beams subjected to different loads (bending, shear, crushing) and made of non-linear materials can be found in Lee (2002) and Teng and Wierzbicki (2003) and references therein. However, no analytical solution is available in the literature for the stiffness of a curved beam subjected to axial load including the effect of large displacements, and this study aims at covering this gap.

2. Problem formulation

The problem under consideration belongs to a class of elastic beam problems which are known to be integrable and is depicted schematically in Fig. 2, where the initial and the deformed configurations are shown for the curved beam subjected to an axial load P along the horizontal axis. Subscript 0 in any magnitude stands for the initial, undeformed beam, while variables without this subindex refer to the deformed configuration. The initial beam length is $2l_0$ and increases to $2l$ during deformation. The positions of a given

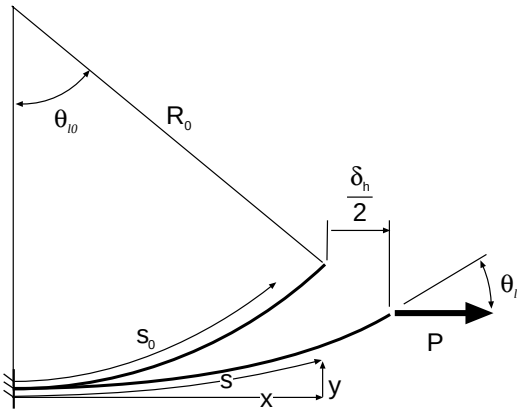

Fig. 2. Diagram showing the initial and deformed beam configurations.

section of the beam in the initial and in the deformed configuration are identified, respectively, by the curvilinear coordinates s_0 and s along the beam or by the corresponding pairs of cartesian coordinates (x_0, y_0) and (x, y). The initial curvature of the beam is constant and equal to $1/R_0$ and the beam is progressively straightened under the action of the external load P. The axial stiffness of the beam, which changes continuously during deformation, can be computed once the horizontal displacement of the beam end, $\delta_h = 2x(l) - 2x_0(l_0)$, is expressed as a function of the applied load, and this is the objective of the mathematical analysis. It is assumed that the beam material behaves as a linear elastic solid characterized by its elastic modulus E, and that the effect of shear deformation can be neglected.

The bending moment, M, at a distance s from the beam center can be expressed as $M = P[y(l) - y(s)]$. The total beam curvature at this section can be computed by adding to the initial curvature $1/R_0$ the contribution due to the bending moment, which is given by

$$\frac{\mathrm{d}\theta}{\mathrm{d}s} = \frac{1}{R_0} - \frac{M}{EI} = \frac{1}{R_0} - \frac{P[y(l) - y(s)]}{EI} \tag{1}$$

according to the Bernouilli–Euler hypothesis, where I is the moment of inertia of the beam section. The bending moment straightens the beam and reduces the curvature, leading to the minus sign in Eq. (1). Differentiating this equation with respect to s and taking into account that $\mathrm{d}y/\mathrm{d}s = \sin\theta$ leads to

$$\frac{\mathrm{d}^2\theta}{\mathrm{d}s^2} = \frac{P}{EI}\frac{\mathrm{d}y}{\mathrm{d}s} = \frac{P}{EI}\sin\theta \tag{2}$$

and this differential equation can be integrated as

$$\frac{1}{2}\left[\frac{\mathrm{d}\theta}{\mathrm{d}s}\right]^2 = -\frac{P}{EI}\cos\theta + C \tag{3}$$

in which C is an integration constant (which depends on P) that can be easily obtained by considering that the radius of curvature should be constant and equal to R_0 when $P = 0$ and that the bending moment at $s = l$ is zero and thus the curvature induced by bending should also be zero. If $\theta(l) = \theta_l$, the curvature can be expressed as

$$\frac{\mathrm{d}\theta}{\mathrm{d}s} = \sqrt{\frac{1}{R_0^2} - \frac{2P}{EI}(\cos\theta - \cos\theta_l)} \tag{4}$$

and the horizontal coordinate of the beam end is given by

$$x(l) = \int_0^l \cos\theta \, \mathrm{d}s = \int_0^{\theta_l} \frac{\cos\theta \mathrm{d}\theta}{\sqrt{\frac{1}{R_0^2} - \frac{2P}{EI}(\cos\theta - \cos\theta_l)}} \tag{5}$$

as a function of θ_l. This equation is transformed after some mathematical manipulation to

$$x(l) = m\sqrt{\frac{EI}{P}}\left\{\left[1 + \frac{2}{m^2}\right]F[\theta_l/2 \mid -m^2] - \frac{2}{m^2}E[\theta_l/2 \mid -m^2]\right\} \tag{6}$$

in which

$$m^2 = \frac{4PR_0^2}{EI - 4PR_0^2 \sin^2\frac{\theta_l}{2}} \tag{7}$$

and $F[\theta_l/2 \mid -m^2]$ and $E[\theta_l/2 \mid -m^2]$ stand, respectively, for the incomplete elliptic integrals of first and second kind. The axial beam displacement, $\delta_h = 2x(l) - 2R_0 \sin\theta_{l0}$ (where $\theta_{l0} = l_0/R_0$) is expressed as

$$\delta_h = 2m\sqrt{\frac{EI}{P}}\left\{\left[1 + \frac{2}{m^2}\right]F[\theta_l/2 \mid -m^2] - \frac{2}{m^2}E[\theta_l/2 \mid -m^2]\right\} - 2R_0 \sin\theta_{l0} \tag{8}$$

and is a function of the applied load P, the bending stiffness EI, and the initial curvature, $1/R_0$. The parameter θ_l in this equation depends on whether the beam length changes upon loading and it is determined below.

2.1. Inextensible beams

If the total beam length remains constant and equal to l_0 during deformation

$$l = l_0 = \int_0^{l_0} \mathrm{d}s = \int_0^{\theta_l} \frac{\mathrm{d}\theta}{\sqrt{\frac{1}{R_0^2} - \frac{2P}{EI}(\cos\theta - \cos\theta_l)}} \tag{9}$$

according to Eq. (4), which leads to

$$l_0 = m\sqrt{\frac{EI}{P}}F[\theta_l/2 \mid -m^2] \tag{10}$$

after some mathematical manipulation. This integral equation can be solved numerically for each value of P to determine the corresponding angle θ_l at the beam end, which is used to compute the horizontal beam displacement.

2.2. Extensible beams

When the beam elongation due to the normal stresses cannot be neglected, each section of the beams undergoes an axial deformation and its length is given by

$$\mathrm{d}s = \left[1 + \frac{P}{E\Omega}\cos\theta\right]\mathrm{d}s_0 \tag{11}$$

where Ω stands for the area of the cross-section. Clearly

$$l_0 = \int_0^{l_0} \mathrm{d}s_0 = \int_0^{l_0} \frac{\mathrm{d}s}{\left[1 + \frac{P}{E\Omega}\cos\theta\right]} \tag{12}$$

and replacing ds by dθ according to Eq. (4), followed by some algebraic transformations, leads to

$$l_0 = m\sqrt{\frac{EI}{P}}\frac{1}{(1+P/E\Omega)}\Pi[n,\theta_l/2 \mid -m^2] \tag{13}$$

where

$$n = \frac{2P}{E\Omega + P} \tag{14}$$

and $\Pi[n,\theta_l/2 \mid -m^2]$ is the incomplete elliptic integral of third kind. The solution of this integral equation provides the angle θ_l at the beam end that can be used to compute the corresponding horizontal beam displacement. Eq. (13) becomes Eq. (10) when $E\Omega/P \to 0$, and the result for inextensible beams is recovered.

3. Results

3.1. Inextensible beams

The evolution of the applied P and the axial beam displacement, δ_h, provided by Eq. (8) for an inextensible beam can be expressed in non-dimensional form using the functions

$$\widehat{P} = \frac{EI\delta_{\max}}{R_0^3} \quad \text{and} \quad \delta_{\max} = 2l_0 - 2R_0\sin\theta_{l0} \tag{15}$$

where $\delta_{\max}$ is the maximum axial displacement of the inextensible beam, attained when the beam is fully extended along the loading axis. These are plotted in Fig. 3 for beams of equal initial length $l_0 = \pi/2$ and radii of curvature $R_0 = 2, 3, 4$, and 8. As expected, the beam axial stiffness increases rapidly during deformation up to infinity as the beam is progressively extended along the loading axis. This variation of the fiber stiffness at the beginning of the deformation controls the initial elastic deformation of polyethylene felts (Chocrón et al., 2002) and it is useful to obtain an accurate and simple analytical expression for the beam behavior, which can be used as the basis for simulation of the elastic deformation of felts. This task requires the previous analysis of the singularity in the curves as $\delta_h \to \delta_{\max}$.

The characteristics of this singularity can be determined by analyzing Eqs. (8) and (10) within the limit $\theta_l \to 0$. For instance, Eq. (10) becomes

$$l_0 = m\sqrt{\frac{EI}{P}}\frac{\theta_l}{2} + \mathrm{O}(\theta_l^3) + \cdots \tag{16}$$

after developing the incomplete elliptic integral of first kind in Taylor power series at $\theta_l \to 0$. Neglecting the third and higher order terms in θ_l and after some mathematical transformations, it can be shown that

$$\lim_{\theta_l \to 0} P = \frac{EI}{R_0^2}\frac{1}{\theta_l^2} \tag{17}$$

Similarly, Eq. (8) becomes

$$\delta_{\max} - \delta_h = 2l_0 - 2m\sqrt{\frac{EI}{P}}\left\{\left[1+\frac{2}{m^2}\right]F[\theta_l/2 \mid -m^2] - \frac{2}{m^2}E[\theta_l/2 \mid -m^2]\right\} \tag{18}$$

Replacing l_0 by the expression given in Eq. (10), followed by developing the elliptic integrals in Taylor power series at $\theta_l \to 0$, and neglecting the fourth and higher order terms in θ_l led to (after a cumbersome mathematical manipulation)

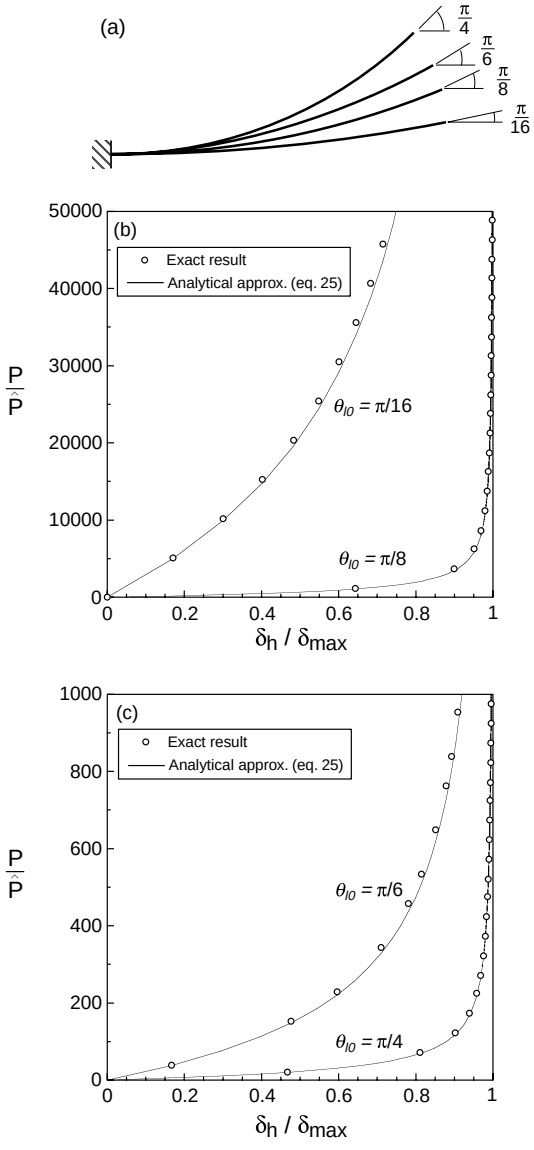

Fig. 3. Non-dimensional plot of the evolution of the beam axial displacement, $\xi = \delta_h/\delta_{\max}$, as a function of the applied load, $P/\widehat{P}$ for inextensible beams of length $\pi/2$. (a) Diagram of the initial shape of the beams indicated by θ_{l0}. (b) Results for beams with initial radius of curvature $R_0 = l_0/\theta_{l0} = 4$ and 8. (c) Results for beams with initial radius of curvature $R_0 = l_0/\theta_{l0} = 2$ and 3. The exact result of Eq. (8) is plotted together with the analytical approximation provided by Eq. (25).

$$\lim_{\theta_l \to 0} (\delta_{\max} - \delta_h) = \frac{R}{2}\theta_l^3 \tag{19}$$

Thus, although P is singular at $\theta_l \to 0$, it is possible to propose a new function $P(1 - \delta_h/\delta_{\max})^{2/3}$ whose limit at $\theta_l \to 0$ is finite and given by

$$\lim_{\theta_l \to 0} P\left(1 - \frac{\delta_h}{\delta_{\max}}\right)^{2/3} = \lim_{\theta_l \to 0} P(1-\xi)^{2/3} = \frac{EI}{2^{2/3} R_0^{4/3} \delta_{\max}^{2/3}} \tag{20}$$

in which $\xi = \delta_h/\delta_{\max}$.

It is easy to obtain an analytical expression for the initial horizontal stiffness of the beam of radius R_0 (which stands for the initial configuration of the curved beam analyzed here, Fig. 2) from linear beam theory. The elastic energy stored in the beam, U, at the beginning of deformation is given by

$$U = 2\int_0^{l_0} \frac{1}{2}\frac{M(s_0)^2}{EI}\,\mathrm{d}s_0 = \int_0^{l_0} \frac{P^2[y(l_0) - y(s_0)]^2}{EI}\,\mathrm{d}s_0 \tag{21}$$

and the initial horizontal displacement, δ_{h0}, can be computed following Castigliano's theorem as

$$\delta_{h0} = \frac{\partial U}{\partial P} = \frac{2PR_0^3}{EI}\phi \tag{22}$$

after some algebra, where ϕ is a constant given by

$$\phi = \int_0^{\theta_{l0}} (\cos\zeta - \cos\theta_{l0})^2\,\mathrm{d}\zeta = \theta_{l0} + \frac{\theta_{l0}}{2}\cos 2\theta_{l0} - \frac{3}{4}\sin 2\theta_{l0} \tag{23}$$

Eq. (22) gives the stiffness of the curved beam at the beginning of deformation ($\xi = 0$) and thus

$$\left.\frac{\mathrm{d}[P(1-\xi)^{2/3}]}{\mathrm{d}\xi}\right|_{\xi=0} = \frac{EI}{2R_0^3\phi}\delta_{\max} \tag{24}$$

and the function $P(1-\xi)^{2/3}$ can be fitted by the minimum squares method to a polynomial function, which is given by

$$\frac{P}{\hat{P}} = \frac{\xi}{2\phi}\frac{1-\beta\xi^2}{(1-\xi)^{2/3}} \quad \text{where} \quad \beta = 1 - 2^{1/3}\phi\left[\frac{R_0}{\delta_{\max}}\right]^{5/3} \tag{25}$$

Eq. (25) provides an accurate fit to the exact solution of $P - \delta_h$ curves given by Eq. (8) for inextensible beams in the whole range of material properties and initial curvatures, as shown in Fig. 3 for beams of length $l_0 = \pi/2$ and radius of curvature in the range 2–8. The maximum error in load predicted by Eq. (25)—as compared to the exact solution of Eq. (8)—is always below 5%, and Eq. (25) can be used confidently to predict the axial stiffness of a curved, inextensible beam.

3.2. Extensible beams

The non-dimensional load–axial displacement curves provided by Eq. (8) for extensible beams are plotted in Fig. 4(a) and (b) for a set of beams of initial length $l_0 = \pi/2$ and radius of curvature $R_0 = 2$ and 8, respectively. The extensibility of the beams in this figure is shown by the non-dimensional parameter $(\Omega/l_0)(R_0^3/I)$, whose value is given in bold characters next to each curve. The inextensible behavior is progressively recovered as this parameter increases.

The beam elongation due to the action of normal forces eliminates the singularity of P at $\xi \to 1$ and the beam axial stiffness departed from the results obtained for inextensible beams. Obviously, the differences between the extensible and inextensible behavior are most significant as ξ approaches 1, and it is sensible to fit the new results by modifying Eq. (25) in this region.

In the case of extensible beams of initial length l_0, the axial stiffness approaches that of a straight column of length l_0 as the beam is fully extended. The elongation of the straight column, $\delta_h - \delta_{\max}$, can be expressed as

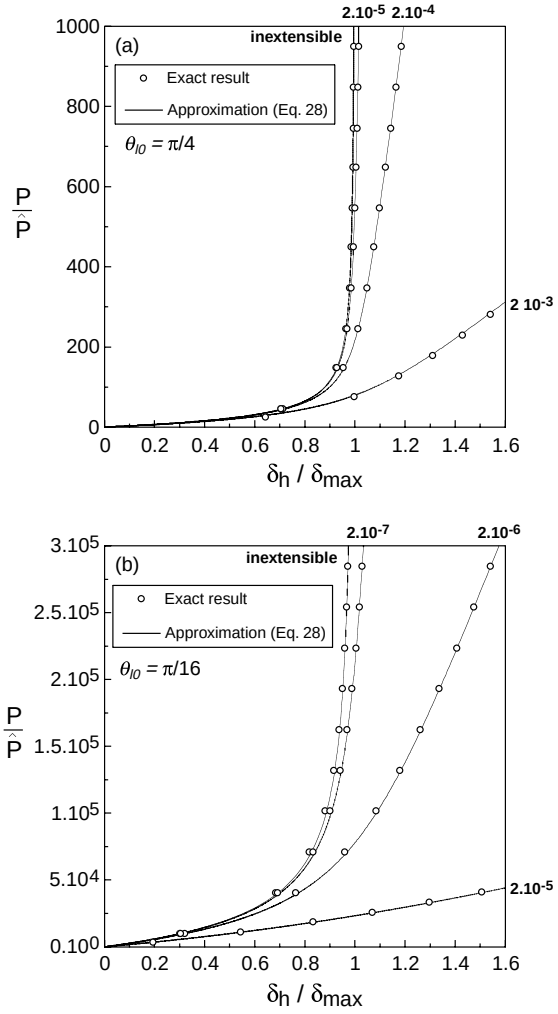

Fig. 4. Non-dimensional plot of the evolution of the beam axial displacement, $\xi = \delta_h/\delta_{\max}$ as a function of the applied load, $P/\widehat{P}$ for extensible beams of length $\pi/2$. (a) Initial radius of curvature $R_0 = l_0/\theta_{l0} = 2$. (b) Initial radius of curvature $R_0 = l_0/\theta_{l0} = 8$. The bold numbers next to each curve stand for the beam extensibility given by $(\Omega/l_0)(R_0^3/I)$. The exact solution of Eq. (8) is plotted together with the analytical approximation of Eq. (28).

$$\delta_h - \delta_{\max} = P\frac{l_0}{E\Omega} \tag{26}$$

The axial displacement of a curved, extensible beam can be approximated by adding the elongation due to bending of an inextensible beam (Eq. (25)) and the axial displacement corresponding to the elongation of a straight column (Eq. (26)). This second term can be expressed in non-dimensional form as $\xi_{\text{ext}} = (\delta_h - \delta_{\max})/\delta_{\max}$, in which the axial elongation due to normal stresses is divided by the maximum axial displacement of the inextensible beam, leading to

$$\xi_{\text{ext}} = \frac{l_0}{\Omega}\frac{I}{R_0^3}\frac{P}{\widehat{P}} \tag{27}$$

which shows that the beam elongation due to normal stresses (normalized by maximum axial displacement due to bending) is controlled by the parameters Ω/l_0 and R_0^3/I, which are related, respectively, to the normal stiffness of the beam section and to the beam axial displacement due to bending. Finally, the total beam elongation can be computed as

$$\xi = \xi_{\text{in}} + \xi_{\text{ext}} = \xi_{\text{in}} + \frac{l_0}{\Omega}\frac{I}{R_0^3}\frac{P}{\widehat{P}} \tag{28}$$

where ξ_{in} is obtained by solving the equation

$$\frac{P}{\widehat{P}} = \frac{\xi_{\text{in}}}{2\phi}\frac{1-\beta\xi_{\text{in}}^2}{(1-\xi_{\text{in}})^{2/3}} \tag{29}$$

and the approximation provided by Eq. (28) is compared with the exact numerical results in Fig. 4. The analytical—although implicit—fit of Eq. (28) is again excellent even in the cases where the beam elongation is important to determine the axial stiffness.

4. Conclusions

An analytical expression is obtained for the axial displacement of a curved, inextensible elastic beam subjected to axial load. The beam deformation was determined from the Bernouilli–Euler hypothesis and included the effect of large displacements. The evolution of the axial displacement as a function of the applied load was expressed in terms of two incomplete elliptic integrals and presented a singularity as the beam was fully extended along the loading axis. The nature of the singularity was determined and the load–axial displacement curves were accurately fitted to a polynomial expression with the same type of singularity, which provides the evolution of the beam stiffness during deformation. Following the same procedure, the behavior of an extensible beam, where the elongation due to the normal stresses cannot be neglected, was also obtained, and the corresponding load–axial displacement curves were fitted to another analytical expression—although implicit—derived from the one developed for inextensible beams.

References

Bisshopp, K.E., Drucker, D.C., 1945. Large deflection of cantilever beams. Quarterly of Applied Mathematics 3, 272–275.

Chocrón, S., Pintor, A., Cendón, D., Roselló, C., Sánchez-Gálvez, V., 2002. Characterization of fraglight non-woven felt and simulation of FSP' impact in it. Report A052804 from the Polytechnic University of Madrid to the U. S. Army.

Cox, H.L., 1952. The elasticity and strength of paper and other fibrous materials. British Journal of Applied Physics 3, 72–79.

DSM, 2004. http://www.dsm.com/.

E.I. DuPont de Nemours Inc., 2004. Available from: <http://www.tyvek.com/>.

Frisch-Fay, F., 1962. Flexible bars. Butterworth & Co., London.

Lee, K., 2002. Large deflections of cantilever beams of non-linear elastic material under a combined loading. International Journal of Non-linear Mechanics 37, 439–443.

Ostoja-Starzewski, M., Stahl, D.C., 2000. Random fiber networks and special elastic orthotropy of paper. Journal of Elasticity 60, 131–149.

Perkins, R.W., 2001. Models describing the elastic, viscoelastic and inelastic mechanical behavior of paper and board. In: Mark, R.E., Habeger, C.C., Borch, J., Lyne, M.B. (Eds.), Handbook of Physical Testing of Paper. Marcel Dekker, New York, pp. 1–76.

Teng, X., Wierzbicki, T., 2003. Crush response of an inclined beam. Thin-Walled Structures 41, 1128–1158.

Van den Akker, J.A., 1962. Some theoretical considerations on the mechanical properties of fibrous structures. In: Bolam, F. (Ed.), The Formation and Structure of Paper. British Paper and Board Makers Association, pp. 205–241.